Earth and Planetary Science Letters 495 (2018) 242–250

Contents lists available at ScienceDirect

Earth and Planetary Science Letters

www.elsevier.com/locate/epsl

Calcium and neodymium radiogenic isotopes of igneous rocks: Tracing crustal contributions in felsic magmas related to super-eruptions and continental rifting

Ryan D. Mills [a,b], Justin I. Simon [a], Donald J. DePaolo [c]

[a] Center for Isotope Cosmochemistry and Geochronology, Astromaterials Research and Exploration Science Division, XI-3, NASA-Johnson Space Center, Houston, TX 77058, USA

[b] Department of Geological Sciences, University of North Carolina at Chapel Hill, Chapel Hill, NC 27599, USA

[c] Department of Earth and Planetary Sciences, Center for Isotope Geochemistry, University of California, Berkeley, CA 94720, USA

ARTICLE INFO

Article history:
Received 31 January 2018
Received in revised form 5 May 2018
Accepted 7 May 2018
Editor: F. Moynier

Keywords:
radiogenic isotopes
calcium
neodymium
felsic magmas

ABSTRACT

Radioactive decay of ^{40}K within the continental crust produces a unique Ca isotopic reservoir, with measurable radiogenic ^{40}Ca excesses compared to Earth's mantle (εCa = 0). Thus, igneous rocks with values of εCa > 1 unambiguously indicate a significant old, crustal contribution to their source magma. At our current level of analytical precision, values of εCa < 0.5 are indistinguishable from mantle-like Ca isotope compositions. So, whereas ^{40}Ca excesses clearly define crustal contributions, the source contributions of igneous rocks with mantle-like Ca isotopic composition are less certain. The calcium in these rocks could be derived from partial melting of: young crust, crust with mantle-like K/Ca compositions, or the mantle itself. Here we present Ca isotopic measurements of intermediate to felsic igneous rocks from the western United States, and two crustal xenoliths found within the Fish Canyon Tuff (FCT) of the southern Rocky Mountain volcanic field (SRMVF), USA. Their isotope geochemistry is used to explore their source compositions and to help distinguish new mantle-derived additions to the crust from reworked older crust.

Irrespective of age or tectonic setting a majority of the intermediate to silicic igneous rocks studied exhibit mantle-like Ca isotope compositions. Mantle-like Ca isotopic data for leucogranites associated with the beginning of Rio Grande rifting in Colorado indicate that felsic melts were generated from newly formed lower crust related to earlier calc-alkaline magmatism. These data also indicate that the Nd isotopic signature in early rift magmas is controlled by the lithospheric mantle, even if the major mantle source reservoir is the asthenospheric mantle.

The two crustal xenoliths found within the 28.2 Ma FCT yield εCa values of 3.6 and 7.0, respectively. The ^{40}Ca excesses of these Precambrian source rocks are supported by K–Ca geochronology. However, like several other ignimbrites from the SRMVF and from Yellowstone, USA, the FCT (εCa ∼ 0.3) has a Ca isotope composition that is indistinguishable from the mantle. Nd isotopic analyses of the FCT imply that it was generated from 10–75% of an enriched component, and so the Ca isotopic data appear to restrict that component to newly formed lower crust, low K/Ca crust, or enriched mantle. Contrary to these findings, several large ignimbrites and one granitoid from the SRMVF show significant ^{40}Ca excesses. These tuffs (Wall Mountain, Blue Mesa, and Grizzly Peak) and one granitoid (Mt. Princeton) are sourced from near, or within the Colorado Mineral Belt. Collectively, these data indicate that felsic, Precambrian crust likely contributed less than 50% of the material to the petrogenesis of many of the large ignimbrites that have erupted across the western United States. However, the crustal components that contributed to magmas in the Colorado Mineral Belt have ^{40}Ca excesses; consistent with felsic, Precambrian crust.

1. Introduction

Oceanic igneous rocks have compositions and isotopic signatures that indicate they are derived from partially melting mantle sources. The sources of felsic magmas erupted through, or emplaced in continental crust are less clear. Evidence for crustal calcium in some oceanic island arcs has been reported in the early studies of Marshall and DePaolo (1989), but resolved at levels that were near the analytical capabilities available at that time. The petrogenesis of felsic magmas in the continental crust can involve,

E-mail address: rdmills@unc.edu (R.D. Mills).

https://doi.org/10.1016/j.epsl.2018.05.017
0012-821X/

in addition to melting of mantle rocks, partial melting of existing crust, fractional crystallization, magma mixing, and assimilation (bulk and selective). The relative importance of these different processes can vary during magma genesis in part due to differences in the thermal structure of the crust and the mass influx from the underlying mantle (DePaolo, 1981; Jellinek and DePaolo, 2003; Annen et al., 2006). It is important to understand how these different processes operate in order to develop planetary differentiation models that accurately account for the formation of new crust and crust-mantle interactions as continents age. Also, looking at younger systems, which generally have been affected less by metamorphic processes, is useful for establishing guidelines that can be applied to older, less well-preserved rock sequences.

Trace element radiogenic isotopes (namely Nd, Sr, and Pb) have long been used to assess the sources of magmas and the role of assimilation–fractional crystallization (i.e. AFC) processes in magma differentiation. In fact, a Nd crustal index (NDI) that calls upon the strength of thermal and mass influx has been proposed (Perry et al., 1993). Significant isotopic variability may (e.g., Gray et al., 2008) or may not (e.g., Coleman et al., 1992) be present in compositionally diverse magma systems. At a larger scale, regional trends can be strong (Farmer and DePaolo, 1983) and likely tied to large tectonic features and crust of different ages. The addition of Os isotopic data has been useful for working on these problems because it can indicate lower crust involvement in magma genesis (Hart et al., 2003). Hafnium isotopes have also proven to be useful for direct comparison to Nd, and Hf in zircon (Kemp et al., 2007) is useful when whole-rock compositions are disturbed (cf. Stelten et al., 2013; Simon et al., 2014). However, given all these tools, there are still many unresolved issues regarding the petrogenesis of felsic magmas, with a principal one being the ability to distinguish the contributions of mantle sources in magmas that clearly have a large component derived from preexisting continental crust.

Of the major elements in igneous rocks, calcium is unique because its most abundant isotope (^{40}Ca) is one of the two daughter products from the branched decay of ^{40}K, another major element. Thus, measuring the ^{40}Ca enrichment in felsic igneous rocks can help assess the involvement of older, K-rich crustal rocks in the petrogenesis of magmas without relying on knowledge of the trace element behavior (e.g., distribution coefficients for Rb and Sr). In addition, because ^{87}Rb/^{87}Sr (parent/daughter) is approximately 30,000 times ^{40}K/^{40}Ca (parent/daughter), the Rb–Sr system has much more variability, which is useful for analyzing diversity, but creates complexities when distinguishing mantle from crust, and necessitates very accurate age corrections for high Rb/Sr rocks. Combining Nd isotopic ratios with Ca isotopic ratios is useful because whereas non-radiogenic Nd can be indicative that either old continental crust or lithospheric mantle was involved in the petrogenesis, Ca isotopes can potentially distinguish between crustal and lithospheric mantle sources (Fig. 1).

This contribution builds on work from Marshall and DePaolo (1989), which used the K–Ca system to trace crustal recycling in felsic magmas from the western United States. Here we report an expanded data set obtained from felsic volcanic and plutonic rocks from the western United States. In addition, we present documentation of a well-defined offset between the standard reference material for Ca (SRM 915a) and rocks representative of Earth's mantle, as well as new methods for analysis of 6 Ca isotopes by Thermal Ionization Mass Spectrometry (TIMS) with long-term external reproducibility of $<0.5\varepsilon$ (2σ) on the ^{40}Ca/^{44}Ca measurement.

2. Methods

Calcium isotopic measurements reported here are from unspiked samples using TIMS. Approximately one-third of the data

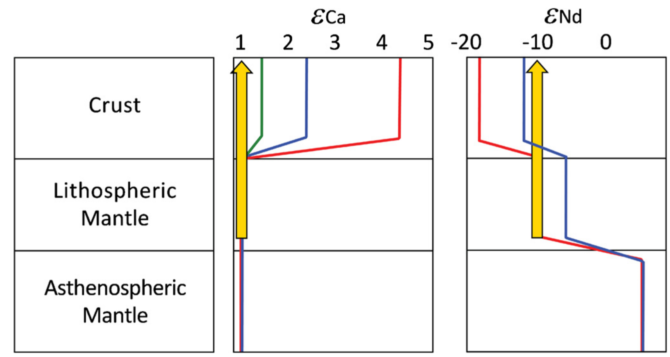

Fig. 1. Schematic diagram illustrating potential Ca and Nd isotopic signatures from the asthenospheric mantle, lithospheric mantle, and crust. Colored lines show hypothetical magma generation paths and the large yellow arrows show that with Nd isotopes it is often difficult to distinguish lithospheric mantle from crust. The combined usage of Ca and Nd isotopes provides greater clarity into the involvement of old felsic crust. (For interpretation of the colors in the figure(s), the reader is referred to the web version of this article.)

collected for this study were obtained at UCB employing the sample handling and mass spectrometry described in Simon et al. (2009). Significant effort has been made to improve upon these methods and to accurately integrate the data from UCB with those obtained at NASA Johnson Space Center (JSC), Fig. 2.

2.1. JSC sample digestion and Ca purification methods

Whole-rock samples (∼50 mg) were powdered with an agate mortar and pestle and dissolved in a combination of concentrated HNO_3 and HF in pressurized dissolution vessels at 180 °C for 48 to 72 h. After pressurized dissolution the acid-sample mixtures were dried and dissolved in HNO_3, if any insoluble material was present the mixture was evaporated to dryness again and dissolved in HNO_3; and this process was continued until all material was in solution. A portion of this solution was then evaporated to dryness and dissolved in dilute HNO_3 and Ca was purified with cation exchange chromatography using a vacuum box following procedures similar to Pourmand and Dauphas (2010). Ca blank introduced during dissolution and column chemistry was approximately 50 ng, approximately 1/20th to 1/30th of this is loaded for an individual run (∼3 μg of sample to ∼2 ng of blank per run). Loading blank was less than 1 ng. Thus, the total Ca blank is not affecting the isotope measurements of the unknowns at our level of precision.

Samples were analyzed using Thermo-Finnigan Triton multicollector mass spectrometers at the University of California at Berkeley (Simon et al., 2009) and at the Lyndon B. Johnson Space Center in Houston (see Table S1).

2.2. JSC mass spectrometer and data reduction methods

During loading, a parafilm "dam" was used to tightly control the location of the sample on the filament. Phosphoric acid was first applied to the center of Re filaments and dried, then approximately 3 μg of Ca in dilute HCl was applied to the filament and dried, finally another application of phosphoric acid was applied and dried. Filament configuration consisted of two filaments (ionization and evaporation) in face-to-face geometry. Ionization filament temperature was continually monitored and kept as close to 1450 °C as possible (±5 °C). These conditions are critical to ion beam stability, removal of volatile K, and staying below source temperatures where Ti ionizes. Evaporation filament current ranged from 1800 to 2200 mA.

Multidynamic analyses involved measurement of ^{39}K, ^{40}Ca, ^{42}Ca, ^{43}Ca, ^{44}Ca, ^{46}Ca, and ^{48}Ca, in three different lines (Table S1) using Faraday collectors with 10^{11} Ω resistors. ^{47}Ti was measured

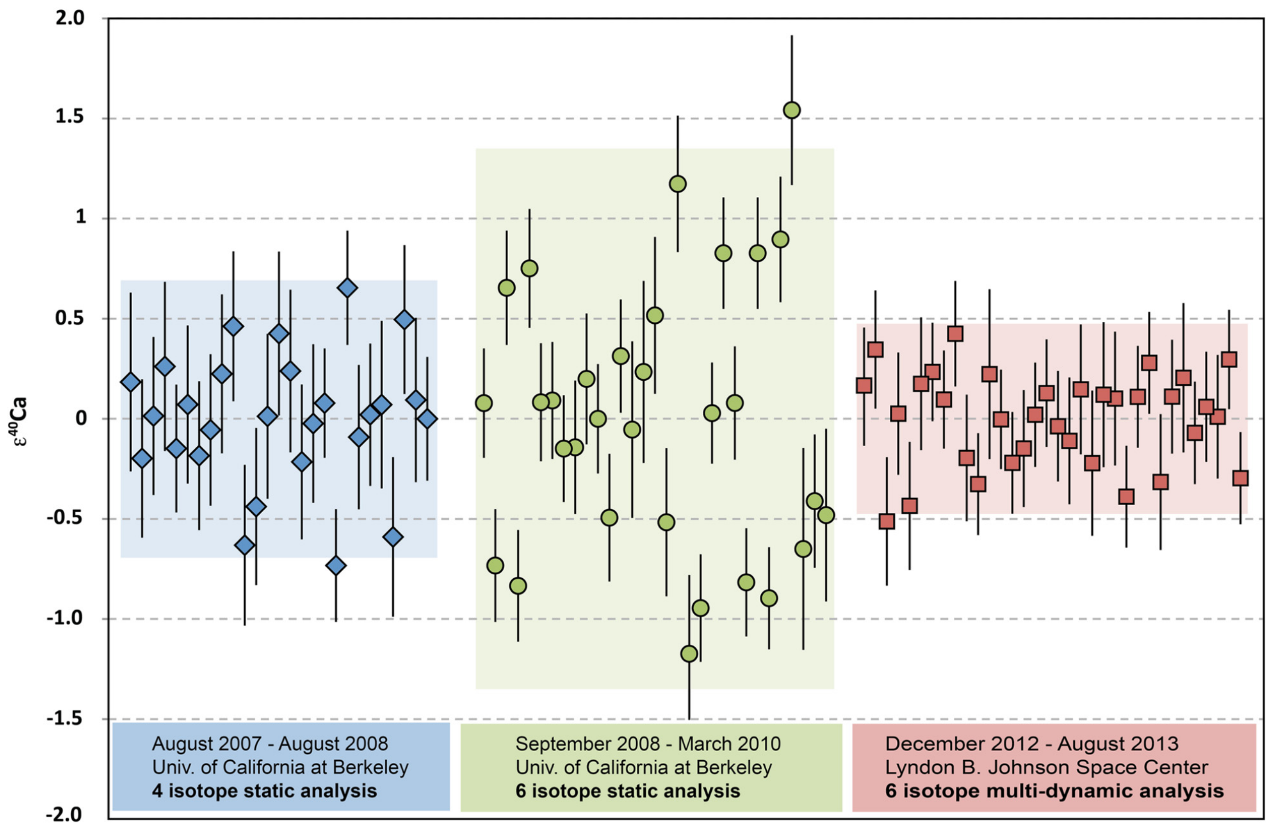

Fig. 2. ε^{40}Ca for the standard SRM 915a from 2007 through 2013.

Table 1
Calcium isotope data.

Sample	Material	Location of analyses	*n*	Age (Ma)	K/Ca	ε^{40}Ca/^{44}Ca[a]	ε^{40}Ca/^{44}Ca[b]	ε^{40}Ca/^{44}Ca[c]	2σ	2σ[d]	MSWD
Ultramafic and mafic rocks											
TP-12	Peridotite	JSC	8			−0.64	0.06		0.25	0.47	0.3
Mantle	Basalts and peridotites	JSC and UCB	23; 5 samples			−0.70	0.00		0.51		1.0
Felsic rocks											
Colorado											
MPRM-15	Wall Mountain Tuff	JSC	4	37	6.50		1.58	1.47	0.36	0.47	5.7
MPRM-17	Quartz monzonite	JSC	2	35	1.35		1.02	0.99	0.44	0.47	4.3
MPRM-23	Leucogranite	JSC	3	30	9.73		0.20	0.03	0.23	0.47	1.6
MPRM-37	Leucogranite	JSC	2	31	8.73		−0.42	−0.58	0.49		4.7
MPRM-38	Leucogranite	JSC	3	31	8.20		0.05	−0.10	1.38		63.4
GU15-08	Grizzly Peak Tuff	JSC	3	34	2.50		1.42	1.37	0.17	0.47	1.0
MLX-3	Granitic xenolith	JSC and UCB	4	1000	2.37		6.99		0.54		6.6
MLX-8	Granitic xenolith	UCB – 4 isotope	3		1.67		3.58		0.94		25.1
Tsag-2g	Saguache Creek Tuff	UCB – 4 isotope	2	32	9.77		0.33	0.17	0.64	0.67	7.5
Tbm-5B	Blue Mesa Tuff	UCB – 4 isotope	3	29	8.93		2.15	2.00	1.04		9.5
Wyoming											
LCT-3a	Lava Creek Tuff	UCB – 4 isotope	4	0.6	8.40		0.32	0.32	0.61	0.67	9.6
HRT-2	Huckleberry Ridge Tuff	UCB – 4 isotope	1	2	3.33		−0.11	−0.11	0.17	0.67	
YCV14	Dry Creek flow	UCB – 4 isotope	3	0.16			1.23	1.23	0.45	0.67	3.5
YCV09	West Yellowstone flow	UCB – 6 isotope	2	0.12			1.99	1.99	1.26	1.35	8.0
YCV04	Solfatara Plateau flow	UCB – 6 isotope	2	0.11			0.39	0.39	1.80		1.4
YCV12	Pitchstone Plateau flow	UCB – 6 isotope	3	0.07			−0.37	−0.37	1.67		4.4
Reference material											
SRM 915a	Carbonate standard	UCB – 4 isotope	34			0 ± 0.67 (2σ)					
SRM 915a	Carbonate standard	UCB – 6 isotope	31			0 ± 1.35 (2σ)					
SRM 915a	Carbonate standard	JSC – 6 isotope	34			0 ± 0.47 (2σ)					

[a] Referenced to SRM 915a.
[b] Referenced to mantle as defined by ultramafic rocks and oceanic basalts; 0.7ε less than SRM 915a.
[c] Age-corrected values.
[d] Uncertainty used if sample uncertainty was lower than standard reproducibility.

to monitor potential ^{48}Ti interferences on a fourth line using a SEM. Evaluating and eliminating interferences at mass 48 are critical for mass dependent double tracer (42–48) work (e.g., Simon and DePaolo, 2010; Simon et al., 2017) and astromaterial studies that seek to assess isotopic anomalies (e.g., Simon et al., 2009; Moynier et al., 2010; Dauphas et al., 2014; Schiller et al., 2015). ^{40}Ca/^{44}Ca values were normalized using a ^{42}Ca/^{44}Ca value of 0.31221 (Russell et al., 1978). 7 blocks of 15 cycles were collected during a given run. Approximately 3 to 5 standards (SRM 915a) were run per sample wheel of 21 loads. Unknowns were referenced to the average ^{40}Ca/^{44}Ca$_n$ of the SRM 915a values for the sample wheel. The reproducibility of the standard per wheel is approximately $\pm 0.5\varepsilon$ (2SD, $n = 34$) (Fig. 1). Unknowns were generally run between 2 and 4 times. Unknowns are directly compared to the 3 to 5 SRM 915a analyses on each sample wheel. Both the weighted means along with the uncertainties on the weighted means are reported in Table 1. By reporting the data in this manner, the relative uncertainties from counting statistics are still important but the absolute magnitudes of the uncertainties on individual analyses have little leverage on the weighted mean and the uncertainty on the weighted mean. The individual uncertainties do become significant for the mean square weighted deviation (MSWD) values shown in Table 1. The primary control of the uncertainty on the weighted mean is the reproducibility of the n replicates.

3. Results

3.1. Calcium isotopic data

Calcium isotopic data presented for 17 samples (Table 1). The results are displayed in ε notation using the following equation (1).

$$\varepsilon_{Ca} = 10^4\left(\frac{^{40}\text{Ca}/^{44}\text{Ca}_{sample}}{^{40}\text{Ca}/^{44}\text{Ca}_{standard}} - 1\right) \quad (1)$$

All samples except the Huckleberry Ridge Tuff (HRT), Wyoming, were analyzed multiple times, ranging from 2 to 8 replicates. The 2σ uncertainty on the weighted mean is shown for all samples with replication, and the in-run precision is shown for the HRT. If the uncertainty is less than the reproducibility of the standard (0.47ε) then the uncertainty of the standard is used for the sample. A MSWD is presented for all samples that were analyzed more than once.

Calcium isotopic results are reported as weighted means of n replicate analyses with the 2σ uncertainty on the weighted mean (Table 1). The unknowns are referenced to Earth's mantle (i.e. $\varepsilon = 0$). From 8 analyses of the Trinity Peridotite (TP-12; sample from Stein Jacobsen, Harvard University) an offset in ε_{Ca} with SRM915a of 0.64 ± 0.47 (2sd) was determined. Combining those data with data from 4 oceanic basalts from Simon et al. (2009) we obtain a 0.7 ± 0.5 (2sd; $n = 23$) difference in ε_{Ca} between Earth's bulk silicate mantle and SRM 915a (Fig. 3). This offset is consistent with values from Simon et al. (2009) that show a similar offset between SRM 915a and achondrite meteorites and measurements from He et al. (2017) who reported a difference of 0.79 between basalts and peridotites and SRM 915a. A similar difference was also reported by Yokoyama et al. (2017). Thus, this offset between the commonly used carbonate standard and bulk silicate planetary materials is found in four different laboratories, on five different TIMS instruments, using different standard and rock powders suites, and by distinct analytical procedures including both static and multi-dynamic approaches.

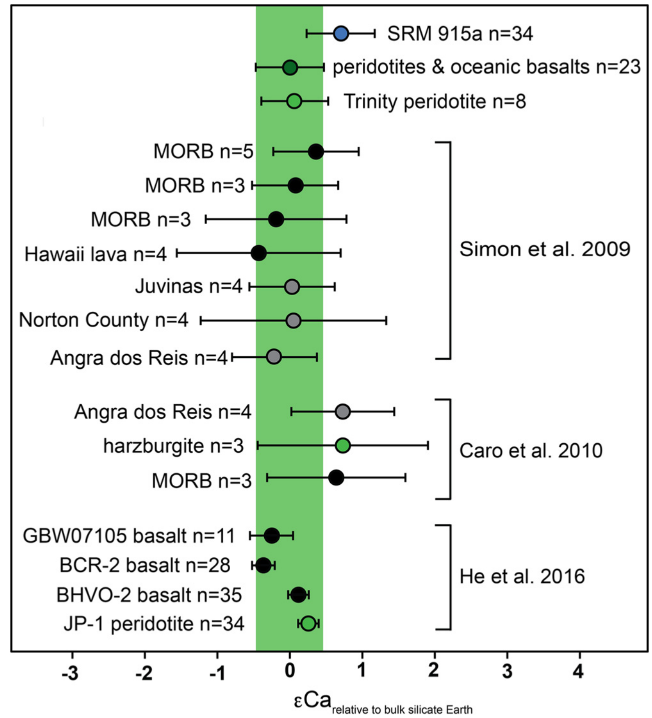

Fig. 3. Plot of ε^{40}Ca showing the carbonate standard (SRM 915a) and materials that should approximate the lowest ε^{40}Ca in the solar system. Data from the Trinity peridotite (this study) and data from Simon et al. (2009) for oceanic basalts are combined to give the zero-value defined as bulk silicate Earth (vertical green band matches the uncertainty in our bulk silicate Earth estimate). The SRM 915a data from this study is 0.7 ε-units higher than bulk silicate Earth. He et al. (2017) reported a difference of 0.79 ε-units between SRM 915a and mean of their basalt and peridotite measurements. Data from Caro et al. (2010) and He et al. (2017) from rocks that should represent 0 ε^{40}Ca are also plotted. Only samples with at least 3 replicates were plotted from Caro et al. (2010). Uncertainties for samples from Caro et al. (2010) are calculated following methods outlined in Simon et al. (2009) using a student-T multiplier. If those calculated uncertainties were lower than the reproducibility of the standard then the reproducibility of the standard was used: 0.47 ε-units (this study), 0.61 ε-units (Simon et al., 2009), and 0.34 ε-units (Caro et al., 2010).

3.2. Colorado

Two granitic xenoliths extracted from the Fish Canyon Tuff (28.2 Ma) that may represent Precambrian basement source components (Bachmann, 2001) have large ^{40}Ca excesses with ε_{Ca} values of 3.58 and 6.99 (Table 1, Fig. 4). In hand sample, they exhibit a mildly penetrative petrofabric defined by a ∼1–5 mm-sized granoblastic mineral assemblage of feldspars, quartz, amphibole, and oxides. Coordinated K–Ca geochronology indicates that one of the xenoliths (MLX-3) is approximately 1 Ga (supplemental material) which is consistent with ages of other Precambrian granitoids in central Colorado (e.g. Pikes Peak Granite, Marshall and DePaolo, 1982). The ε_{Ca} values of these crustal xenoliths clearly show the effects of ^{40}K decay, but their high K/Ca ratios may not be representative of the bulk of the lower half of the continental crust. For comparison, we note that typical granodioritic crustal rocks with K/Ca ratios in the range 0.3 to 1.0 and ages of about 1.8–2.0 Ga might typify the basement rocks under most of Colorado, and would have had ε_{Ca} values of about 0.6 to 2.2 at the time of formation of the Fish Canyon Tuff, but also would have had higher Ca concentrations than the xenoliths.

In contrast to the granitic xenoliths, and the other estimates for crustal rocks, the Fish Canyon Tuff ($\varepsilon\text{Ca}_{(t)} = 0.27 \pm 0.61$; Simon et al., 2009) does not have elevated ε_{Ca}. The Saquache Creek Tuff (32 Ma; Lipman and McIntosh, 2008; Simon, 2000), another large-

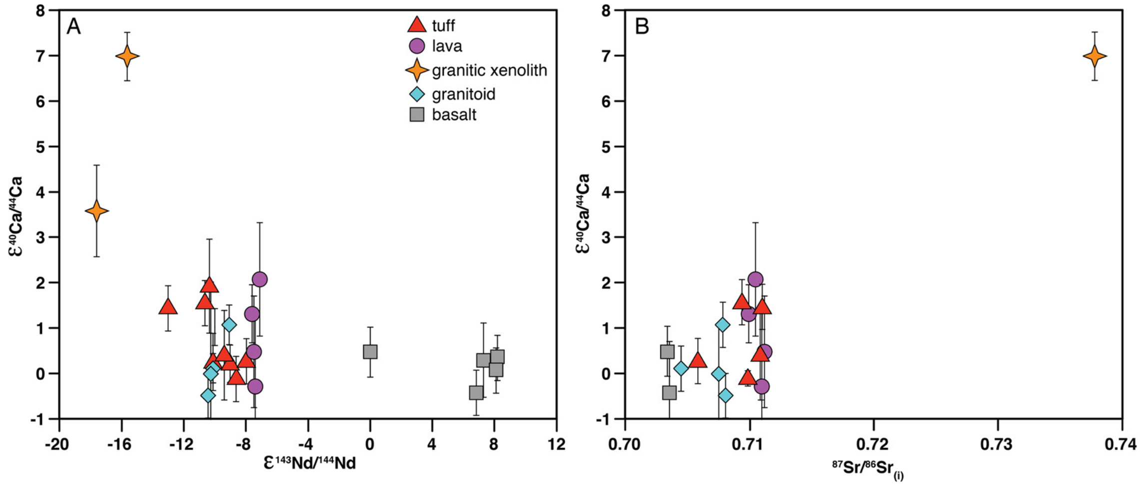

Fig. 4. (A) Plot of ε^{143}Nd vs ε^{40}Ca. (B) Plot of $^{87}Sr/^{86}Sr_{(i)}$ vs ε^{40}Ca. Basalt data are from Simon et al. (2009). Epsilon values for Nd were calculated using $^{143}Nd/^{144}Nd$ (CHUR, 0 Ma) = 0.512638 and $^{147}Sm/^{144}Nd$(CHUR, 0 Ma) = 0.1967.

volume ignimbrite from the central San Juan volcanic field gives similar results, with $\varepsilon Ca_{(t)} = 0.17 \pm 0.64$.

Other ignimbrites from Colorado (Table 1, Fig. 4) show larger ^{40}Ca enrichments, relative to the Fish Canyon and Saquache Creek tuffs. The Grizzly Peak Tuff (34.3 Ma; McIntosh and Chapin, 2004), which erupted from the Grizzly Peak Caldera inside the Colorado Mineral Belt gives an $\varepsilon Ca_{(t)}$ value of 1.37 ± 0.47. The Wall Mountain Tuff (37.2 Ma; Zimmerer and McIntosh, 2012) which is thought to originate from the Mount Princeton area (Lipman, 2007) also shows significant ^{40}Ca excess ($\varepsilon Ca_{(t)} = 1.47 \pm 0.47$). The Blue Mesa Tuff, likely sourced from the western San Juan volcanic field also shows a ^{40}Ca excess ($\varepsilon Ca_{(t)} = 2.00 \pm 1.04$).

For comparison, four plutonic rocks from the Mount Princeton batholith were also analyzed for Ca isotopes. A quartz monzonite (35.4 Ma; Mills and Coleman, 2013) is enriched in ^{40}Ca with an $\varepsilon_{Ca(t)}$ value of 0.99 ± 0.47. Three ∼30 Ma leucogranites from the batholith (Zimmerer and McIntosh, 2012; Mills and Coleman, 2013) all have similar calcium isotopic compositions, and all of the values within uncertainty of Earth's mantle (Table 1, Fig. 4).

3.3. Wyoming

We present data for six volcanic rocks from the Yellowstone caldera system, USA. Samples from the Lava Creek Tuff (627 ka, Mark et al., 2017) and the Huckleberry Ridge Tuff (2.1 Ma, Ellis et al., 2012) are within uncertainty of the mantle for ε_{Ca}. However, there is diversity in the 4 samples from the Central Plateau Member post-caldera lavas, with $\varepsilon Ca_{(t)}$ ranging up to 2 ± 1, although there are elevated uncertainties on 3 of the 4 samples (Table 1, Fig. 4).

4. Discussion

4.1. Offset between Ca isotope ratio in Earth's mantle and SRM 915a

It has been reported (Caro et al., 2010) that the SRM915a ($CaCO_3$) standard is not enriched in ^{40}Ca relative to bulk Earth, even though those authors claimed to have measurement precision that could detect small differences. Our results, however, indicate that SRM 915a (at least two batches used previously at UC Berkeley and JSC, both measured in this study) contain a measurable ^{40}Ca excess when directly compared to natural silicates used to define planetary values, i.e., bulk silicate Earth. Our determination of a $0.7 \pm 0.5\varepsilon$ difference between Earth's mantle and the standard used by most analysts (SRM 915a) is consistent with a 0.79ε difference reported in He et al. (2017). The elevated $^{40}Ca/^{44}Ca$ of SRM 915a has implications for recent Ca isotope work, and allows for more direct comparison between different laboratories. Caro et al. (2010) present their data as individual measurements, and present replicate measurements for most samples. For samples that have at least 2 replicates their normal reproducibility is similar to ours, with 2SE uncertainty on the weighted means $\sim \pm 0.5\varepsilon$. Recasting their results for oceanic basalts, harzburgite, achondrites, and lunar samples with the 0.7ε offset from SRM 915a shows (Fig. 3) that most of the results of Caro et al. (2010) appear to be shifted to higher ε_{Ca} values, very similar to SRM 915a. However, their samples that arguably best approximate Earth's mantle are also within error of our preferred reference point (i.e. $\varepsilon_{Ca} = 0$).

The fact that the offset we report here, consistent with He et al. (2017), has been found at multiple facilities employing different Triton TIMS instruments, implies that a reevaluation of the dataset of silicates, carbonates, seawater, river water, and extraterrestrial material presented in Caro et al. (2010) may be prudent. The difference between Earth's mantle and SRM915a we present could change the main conclusion of Caro et al. (2010) that the oceanic Ca cycle is minimally affected by Ca from the continental crust over geologic history. Likewise, this shift explains the anomalous meteorite compositions of a recent study that reports ε_{Ca} values lower than SRM915a by ∼0.5 to 1.0ε (Yokoyama et al., 2017).

Additionally, relatively small differences in the "normal" $^{40}Ca/^{44}Ca$ values used in the data reduction calculations of mass dependent Ca isotope studies could produce resolvable differences. For example, the $\sim 0.7\varepsilon$ difference reported here leads to a systematic shift of ∼0.07‰ in a computed $\delta^{40}Ca/^{44}Ca$ value, which is similar to the apparent discrepancy between the average "planetary" or bulk silicate Earth values reported by recent UC Berkeley and Harvard studies (e.g., Simon and DePaolo, 2010 and Huang and Jacobsen, 2017). Mass dependent fractionation studies (e.g., Valdes et al., 2014) employing sample standard bracketing that only measure other calcium isotopes (i.e., ^{42}Ca, ^{43}Ca, and ^{44}Ca) are immune to the excess ^{40}Ca in SRM915a issue.

4.2. Assessing crustal recycling versus mantle additions in continental felsic magmatism

Continental felsic magmas are, in general, mixtures of recycled crust (partial melting) and additions of new melts from the mantle. Understanding the relative proportions of new and recycled crust is a long-standing unknown in geological research (e.g. Perry et al., 1993). In this section we discuss the roles of mantle and crust in felsic magmatism from select locations across the western US

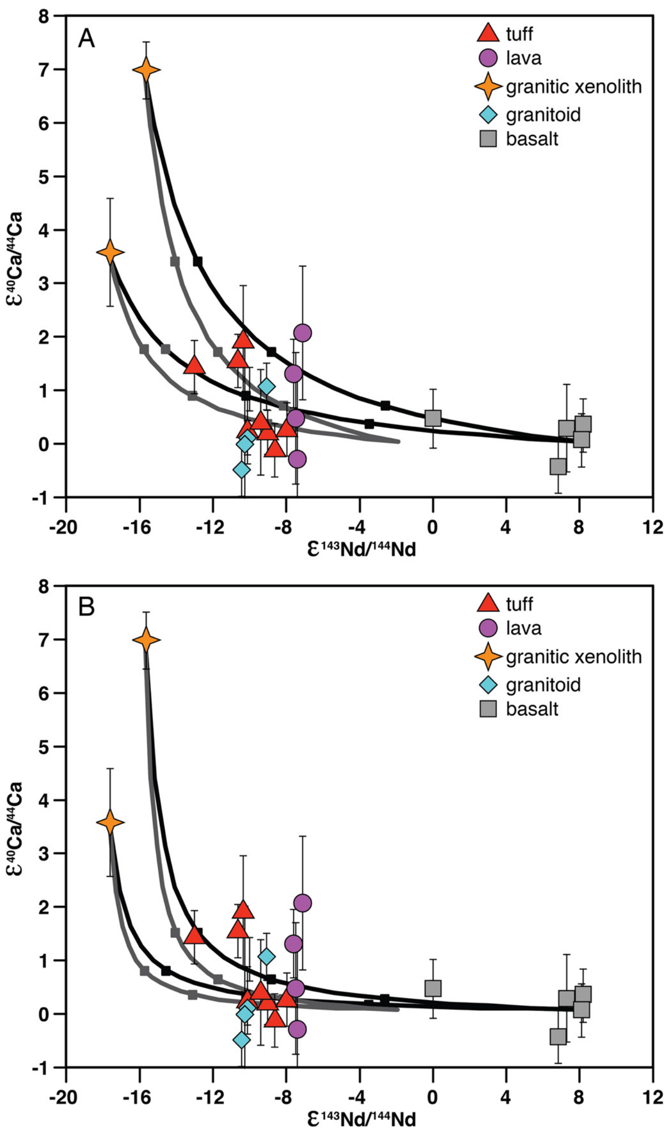

Fig. 5. (A) Plot of ε^{143}Nd vs ε^{40}Ca with four reference mixing models plotted. The end-members for the mixing models are athenospheric mantle [ε^{143}Nd = 8, ε^{40}Ca = 0, [Ca] = 11.3 wt%, [Nd] = 11 ppm], lithospheric mantle [ε^{143}Nd = −2, ε^{40}Ca = 0, [Ca] = 11.3 wt%, [Nd] = 11 ppm], old felsic crust [ε^{143}Nd =-17.6, ε^{40}Ca = 3.6, [Ca] = 3.6 wt%, [Nd] = 27 ppm] [ε^{143}Nd = −15.6, ε^{40}Ca =7.0, [Ca] = 3.6 wt%, [Nd] = 27 ppm]. Ticks on mixing models mark 25% mixing intervals. (B) Plot of ε^{143}Nd vs ε^{40}Ca with four reference mixing models plotted. The end-members for the mixing models are asthenospheric mantle [ε^{143}Nd = 8, ε^{40}Ca = 0, [Ca] = 11.3 wt%, [Nd] = 11 ppm], lithospheric mantle [ε^{143}Nd = −2, ε^{40}Ca = 0, [Ca] = 11.3 wt%, [Nd] = 11 ppm], old high-silica crust [ε^{143}Nd =-17.6, ε^{40}Ca = 3.6, [Ca] = 1.0 wt%, [Nd] = 27 ppm] [ε^{143}Nd = −15.6, ε^{40}Ca = 7.0, [Ca] = 1.0 wt%, [Nd] = 27 ppm]. Ticks on mixing models mark 25% mixing intervals. Basalt data are from Simon et al. (2009).

using whole-rock Ca isotopic data combined with whole-rock Nd isotopic data.

Several isotopic mixing models (Fig. 5) were generated in order to investigate the relative contributions of old, felsic crust and lithospheric and asthenospheric mantle components. Calcium and Nd data for the Precambrian xenoliths from this study were used as the isotopic end-members for old, felsic crust. If estimated lower crustal rock compositions were used, the mixing lines would be slightly different. In our model, there is no difference in εCa between the different mantle reservoirs (asthenosphere and lithosphere). We use εNd of +8 for the asthenospheric mantle (Hofmann, 1997) and −2 for the lithospheric mantle, which is a reasonable estimate for the lithospheric mantle under Colorado

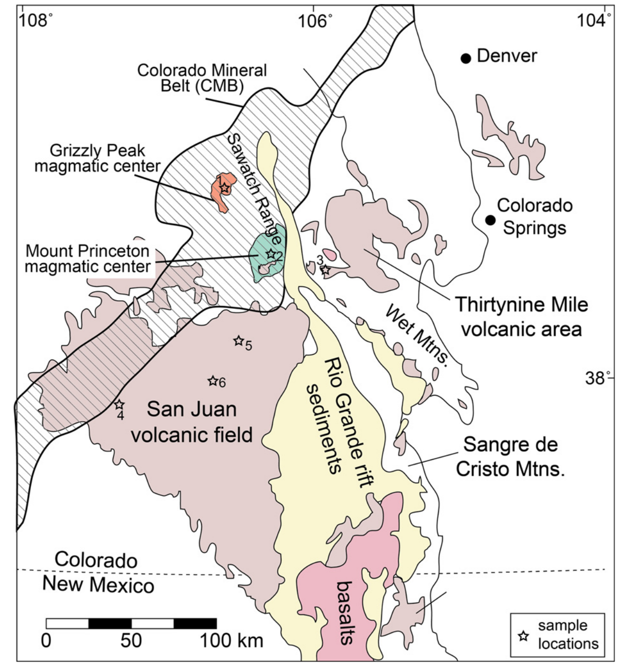

Fig. 6. Map of southern Rocky Mountain volcanic field and surrounding magmatic features in Colorado and northern New Mexico (after Lipman, 2007). Sample locations are listed with numbers; 1= Grizzly Peak Tuff (GU15-08), 2 = Mt. Princeton batholith samples (MPRM-17, -23, -37, -38), 3 = Wall Mt. Tuff (MPRM-15), 4 = Blue Mesa Tuff (Tbm-5B), 5 = Saguache Creek Tuff (Tsag-2g), 6 = granitic xenoliths (MLX-3, -8).

(Jacob et al., 2015). The other variables of the mixing models are the [Ca] and [Nd] for the crust and the mantle. We used two different values for the crust, one is average continental crust (CaO = 3.59 wt%, Nd = 27 ppm; Rudnick and Gao, 2003) and the other is a high-silica composition with CaO = 1 wt% and Nd = 27 ppm. Large database analysis of igneous rocks (Glazner et al., 2015) show more scatter in [Nd] for high-silica rocks, but the average is near continental crust value of Rudnick and Gao (2003), thus 27 ppm is used for consistency. For the mantle we used Ca = 11.3 wt% and Nd = 11 ppm (Hofmann, 1988). Hence the mantle magma Ca/Nd ratio is roughly 8 to 25 times higher than that of the crustal rock compositions we are using for the models. It is important to note that old crust with higher CaO concentrations (e.g. average continental crust) would have lower εCa due to lower bulk K/Ca.

The Tertiary felsic rocks analyzed in this study are interpreted to be the result of mixing between mantle and the old crust as defined by our analyses of Precambrian xenoliths (Fig. 5). The ε_{Nd} values of our Tertiary felsic rock samples are all substantially lower than that estimated for the lithospheric mantle component (Jacob et al., 2015), but higher than the values for the xenoliths, and the values estimated for the crustal provinces they occur in (Bennett and DePaolo, 1987), which are in the range −12 to −15. Three of the rocks, however, have ε_{Nd} values that are quite close to the values estimated for the crust, which then raises the question of whether there is evidence that mantle magma was involved in their generation.

4.2.1. Magmatism in the southern Rocky Mountain volcanic field

The mid-Tertiary southern Rocky Mountain volcanic field (Fig. 6) contains magmatic centers that are dominated by large, caldera-forming ignimbrites (Lipman, 2007). Our data for four large ignimbrites and one granitoid, combined with data for two additional ignimbrites in the region (Simon et al., 2009) show interesting spatial variability. Three ignimbrites sourced from close to the NE–SW trending Colorado Mineral Belt (CMB) (Fig. 6) and one granitoid within the CMB have $\varepsilon Ca_{(t)}$ that is clearly resolvable from and higher than the value for Earth's mantle. Ignimbrites SE of the CMB, including the Fish Canyon Tuff, have $\varepsilon Ca_{(t)}$ within uncertainty of the mantle. Calcium isotope data for USGS rock standard GSP-2, granodiorite sampled from the Silver Plume Quarry inside the CMB, shows a high εCa of 4.04 ± 0.15 (relative to SRM 915a; He et al., 2017), as expected for a Precambrian, felsic igneous rock (∼1.4 Ga).

In order to evaluate this spatial variability, it is important to understand how the CMB may have formed. The two main hypotheses for the generation of the CMB are: 1) magmas were localized along Precambrian shear zones (Tweto and Sims, 1963) and 2) a leaky transform in the underlying flat slab (Farallon plate) provided fluids and heat which melted a linear portion in the overlying lithosphere (Barker and Stein, 1990; Chapin, 2012). Whereas there are local shear zones associated with much of the CMB, young (<75 Ma) structures and distinct magmatic sources between areas north and south of the CMB suggest Precambrian structures cannot solely account for the CMB (Chapin, 2012). Neodymium isotopic data support a model where CMB magmas between 75 and 30 Ma were generated by partial melting of Precambrian felsic and mafic lower crust (± mantle), with more metasomatized mafic crust being the early dominant component (75–45 Ma; Stein and Crock, 1990). Calcium data presented here point to the reworked felsic Precambrian crust as a significant component to the magmas generated in close proximity to the CMB; magmas generated farther to the SE (e.g. Fish Canyon Tuff) appear to have less of that component based on Ca isotopes, but still have low ε_{Nd} values that require substantial contributions from crustal source rocks.

Based on likely mixing scenarios (Fig. 5), the Nd and Ca isotopic data suggest that the high εCa felsic magmas from near the CMB contain 50–70% Precambrian crust and the felsic magmas generated farther to the SE contain smaller fractions, in the range 30–50% Precambrian crust. It should be noted that Perry et al. (1993) recognized a temporal change in the fraction of crust involved in the formation of large volume Cenozoic ignimbrites in the western U.S. Those tuffs with the highest crustal fractions, which include the Grizzly Peak Tuff, are in the range 35–30 Ma, older than the 28 Ma Fish Canyon Tuff. The 37 Ma Wall Mountain Tuff studied here also appears to have a large crustal fraction based on both Nd and Ca isotopes.

4.2.2. Yellowstone caldera

The varied εCa values for the Central Plateau Member (CPM) lavas compared to the uniform values for the Lava Creek Tuff and Huckleberry Ridge Tuff (Fig. 7) suggest that generation of felsic magma with relatively protracted shallow crustal residence lifetimes (CPM, Vazquez and Reid, 2002) may preserve isotopic diversity from crustal source regions, but the large-volume felsic magmas in the area show a dominant lower crustal or mantle component. This is in general agreement with Bindeman and Valley (2000), who showed the preservation of oxygen isotopic diversity in xenocrysts and antecrysts (crystals carried over from previous generations of felsic crustal magma), that is not evident in whole rock samples. The data are also consistent with the idea that isotopic effects are being governed by the dynamics between magma crustal residence time scales and mantle input, as has been suggested for Long Valley, California, another well studied caldera-forming system (Simon et al., 2007, 2014). Another possibility is that the lavas and the large volume tuffs were sourced from different reservoirs, with genesis of the effusive lavas occurring mostly in the felsic, mid- to upper-crust and genesis of the large volume tuffs involving larger proportions of melting of lower crust (e.g. Sisson et al., 2005). Yellowstone may be unique in that the mantle plume source provides a high mantle magma flux that can potentially produce a large volume ignimbrite with a smaller admixture

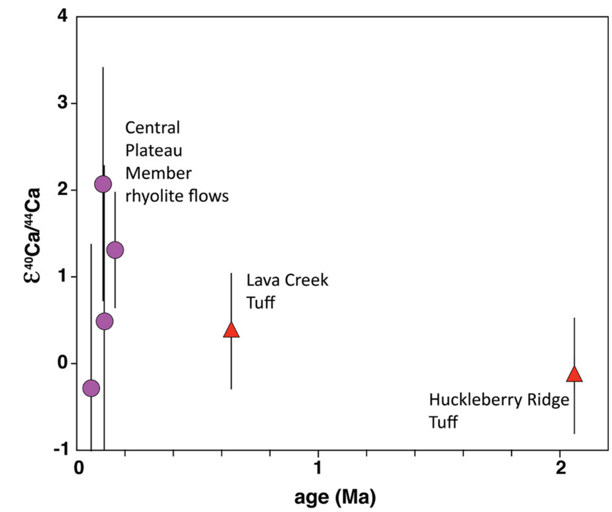

Fig. 7. Plot of ε^{40}Ca vs age for volcanic rocks from the Yellowstone caldera.

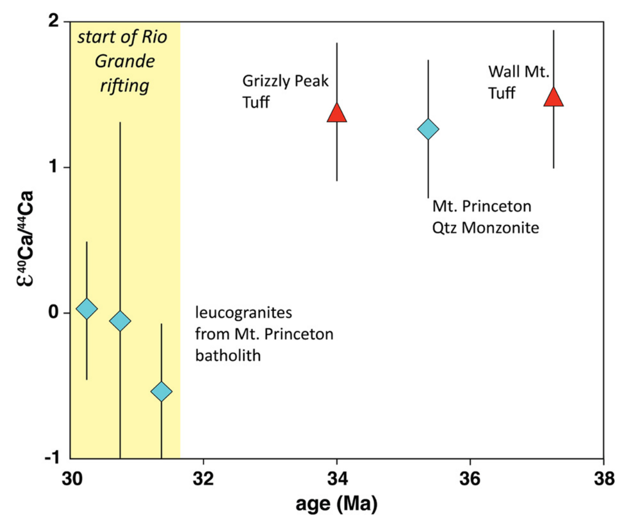

Fig. 8. Plot of ε^{40}Ca vs age for granitoids and ignimbrites from the Sawatch Range in central Colorado.

of lower crustal melting. The other ignimbrites erupting from locations away from the Colorado Mineral Belt (above), suggest that large eruptions that have εCa near zero might have assembled by amalgamation of diverse magma batches, some could have had elevated εCa, but that the majority of the Ca in the magma batches is dominated by Ca from the lower-K/Ca source rocks either in the lower crust or underlying mantle (e.g., Nash et al., 2006).

4.2.3. Felsic magmatism during the onset of continental rifting

Plutonic and volcanic rocks from the Sawatch Range in central Colorado document the onset of lithospheric thinning during the initial stage of Rio Grande rifting (Figs. 6, 8). The Wall Mt. Tuff (37.3 Ma; Zimmerer and McIntosh, 2012), the Mt. Princeton Quartz Monzonite (35.4 Ma; Mills and Coleman, 2013), and the Grizzly Peak Tuff (34.3 Ma; McIntosh and Chapin, 2004) record the calc-alkaline magmatism thought to be related to subduction prior to rifting. The Ca and Nd isotopic data (Fig. 5) indicate that these magmas are a mixture of mantle (likely lithospheric) and continental crust; with εCa values above 1 and εNd between −9 and −13. This differs from the 31–30 Ma leucogranites from the Mt Princeton batholith, thought to represent magmatism associated with early Rio-Grande rifting (Shannon, 1988; Mills, 2012), which have εCa values of 0 and εNd of ∼−10. The lack of elevated εCa in the leucogranites, combined with a negligible shift in εNd from the earlier calc-alkaline magmatism suggests that the crustal component of the leucogranites is different than the crustal component of the calc-alkaline magmas, and that the Nd isotopic budget during early continental rifting is dominated by the lower crust/lithospheric mantle.

We suggest that new lower crust was produced during the earlier calc-alkaline magmatism (37–34 Ma), and partial melts of that new crust are the main source for the leucogranites. Another piece of support for this model is the occurrence of mineralization associated with the leucogranites (Mutschler et al., 1981). The high volatile content needed for the mineralization would have been available in the newly generated lower crust. A simpler model to explain the isotopic data of the leucogranites would be that the lack of an old felsic crustal component in the leucogranites is due to chemical and isotopic diversity in the basement rocks and that the crustal source for the leucogranites was old mafic crust. This model does not explain the high volatile content of the leucogranite system and would require that felsic melts could still be generated from mafic crust that had already been subjected to partial melting during earlier magmatism in the area. Finally, any partial melt of the asthenospheric mantle that was involved in the petrogenesis of the leucogranites did not alter the Nd isotopic signature; this would be expected due to the relative neodymium concentrations of the two mantle reservoirs (i.e., $[\mathrm{Nd}]_{\mathrm{asthenosphere}} < [\mathrm{Nd}]_{\mathrm{lithosphere}}$).

4.3. Implications for the generation of large ignimbrites

There is considerable on-going debate about where in the crust the chemical differentiation that produces large bodies of dacitic to rhyolitic magma occurs.

1. Epsilon Ca of close to zero for some ignimbrites strongly suggests that the parental magma originated from mantle. The Ca isotopic composition is not sensitive to an admixture of crustal rock, but Nd isotopic compositions suggest that these tuffs may contain about 30% or more crustal material.
2. Ignimbrites from near the CMB, all of which are in the older (Oligocene) grouping of Perry et al. (1993) have much larger components of old, felsic crust, mostly greater than 50%.
3. Small volume additions to large ignimbrite magmas may be isotopically diverse but their signal is extremely muted in the final product.

5. Conclusions

Calcium isotopes from felsic igneous rocks show varied enrichment of ^{40}Ca from decay of ^{40}K. Igneous rocks with large excesses (>1 ε-unit) are from continental interiors, where large portions of old crust were recycled during their magma genesis. However, felsic magmas from continental interiors can show no excess ^{40}Ca, indicating that those magmas involved addition of new mantle derived material to the crust during genesis, or they partially melted mafic lower crust. These results show that in the continental interior some magmatic systems recycled up to 70% old crust and some recycled less than 30%, likely depending on the thermal regime and/or chemical composition of the lower crust, and the flux of magma provided from the mantle.

Acknowledgements

We thank Olivier Bachmann, Stein Jacobsen, and Jorge Vazquez for sharing sample materials of crustal xenoliths contained in the Fish Canyon Tuff, peridotite from the Trinity Ophiolite, and Central Plateau Member lavas from Yellowstone, respectively. Helpful comments of Brian Marshall, an anonymous reviewer, and Editor Frederic Moynier are greatly appreciated. Michael Tappa was incredibly helpful with laboratory and analytical work at JSC. Drew Coleman and Ryan Frazer provided informal reviews of the manuscript. Work was partially supported by NASA grants 11-COS11-0066 and 16-EW16_2-0163 to J.I.S, the NASA Postdoctoral Program support to R.D.M, and the Petrology and Geochemistry program of NSF (EAR0408521,0838168 and 100500) to D.J.D.

Appendix A. Supplementary material

Supplementary material related to this article can be found online at https://doi.org/10.1016/j.epsl.2018.05.017.

References

Annen, C., Blundy, J.D., Sparks, R.S.J., 2006. The genesis of intermediate and silicic magmas in deep crustal hot zones. J. Petrol. 47, 505–539.

Bachman, O, 2001. Volcanology, Petrology and Geochronology of the Fish Canyon Magmatic System, San Jan Volcanic Field, U.S.A. Ph.D. Thesis, University of Geneva. 199 pp.

Barker, F., Stein, H.J., 1990. Origin of Laramide magmas of the Colorado Mineral Belt over a leaky transform in the flatly subducted Farallon plate. Abstr. Program – Geol. Soc. Am. 22, 5.

Bennett, V.C., DePaolo, D.J., 1987. Proterozoic crustal history of the western United States as determined by Neodymium isotopic mapping. Geol. Soc. Am. Bull. 99, 674–685.

Bindeman, I.N., Valley, J.W., 2000. Formation of low-δ^{18}O rhyolites after caldera collapse at Yellowstone, Wyoming, USA. Geology 28, 719–722.

Caro, G., Papanastassiou, D.A., Wasserburg, G.J., 2010. ^{40}K–^{40}Ca isotopic constraints on the oceanic calcium cycle. Earth Planet. Sci. Lett. 296, 124–132.

Chapin, C.E., 2012. Origin of the Colorado Mineral Belt. Geosphere 8, 28–43.

Coleman, D.S., Glazner, A.F., Frost, T.P., 1992. Evidence from the Lamarck Granodiorite for rapid Late Cretaceous Crust Formation in California. Science 258, 1924–1926.

Dauphas, N., Chen, J.H., Zhang, J., Papanastassiou, D.A., Davis, A.M., Travaglio, C., 2014. Calcium-48 isotopic anomalies in bulk chondrite and achondrites: evidence for a uniform isotopic reservoir in the inner protoplanetary disk. Earth Planet. Sci. Lett. 407, 96–108.

DePaolo, D.J., 1981. Trace element and isotopic effects of combined wallrock assimilation and fractional crystallization. Earth Planet. Sci. Lett. 53, 189–202.

Ellis, B.S., Mark, D.F., Pritchard, C.J., Wolff, J.A., 2012. Temporal dissection of the Huckleberry Ridge Tuff using the ^{40}Ar/^{39}Ar dating technique. Quat. Geochronol. 9, 34–41.

Farmer, G.L., DePaolo, D.J., 1983. Origin of Mesozoic and tertiary granite in the Western United States and implications for Pre-Mesozoic crustal structure, 1: Nd and Sr Isotopic studies in the Geocline of the Northern Great Basin. J. Geophys. Res. 88, 3379–3401.

Glazner, A.F., Coleman, D.S., Mills, R.D., 2015. The volcanic–plutonic connection. In: Advances in Volcanology.

Gray, W., Glazner, A.F., Coleman, D.S., Bartley, J.M., 2008. Long-term geochemical variability of the Late Cretaceous Tuolumne Intrusive Suite, central Sierra Nevada, California. Geol. Soc. Lond. 304, 183–201.

Hart, G.L., Johnson, C.M., Hildreth, W., Shirey, S.B., 2003. New osmium isotope evidence for intracrustal recycling of crustal domains with discrete ages. Geology 31, 427–430.

He, Y., Wang, Y., Zhu, C., Huang, S., Li, S., 2017. Mass-independent and mass-dependent Ca isotopic compositions of thirteen geological reference materials measured by thermal ionization mass spectrometry. Geostand. Geoanal. Res. 41, 283–302.

Hofmann, A.W., 1988. Chemical differentiation of the Earth: the relationship between mantle, continental crust, and oceanic crust. Earth Planet. Sci. Lett. 90, 297–314.

Hofmann, A.W., 1997. Mantle geochemistry: the message from oceanic magmatism. Nature 385, 219–229.

Huang, S., Jacobsen, S.B., 2017. Calcium isotopic compositions of chondrites. Geochim. Cosmochim. Acta 201, 364–376.

Jacob, K.H., Farmer, G.L., Buchwaldt, R., Bowring, S.A., 2015. Deep crustal anataxis, magma mixing, and the generation of epizonal plutons in the Southern Rocky Mountains, Colorado. Contrib. Mineral. Petrol. 169, 7.

Jellinek, A.M., DePaolo, D.J., 2003. A model for the origin of large silicic magma chambers: precursors to caldera-forming eruptions. Bull. Volcanol. 65, 363–381.

Kemp, A.I.S., Hawkesworth, C.J., Foster, G.L., Paterson, B.A., Woodhead, J.D., Hergt, J.M., Gray, C.M., Whitehouse, M.J., 2007. Magmatic and crustal differentiation history of granitic rocks from Hf–O isotopes in zircon. Science 315, 980–983.

Lipman, P.W., 2007. Incremental assembly and prolonged consolidation of Cordilleran magma chambers: evidence from the Southern Rocky Mountain volcanic field. Geosphere 1, 42–70.

Lipman, P.W., McIntosh, W.C., 2008. Eruptive and noneruptive calderas, northeastern San Juan Mountains, Colorado: where did the ignimbrites come from? Geol. Soc. Am. Bull. 120, 771–795.

Mark, D.F., Renne, P.R., Dymock, R., Smith, V.C., Simon, J.I., Morgan, L.E., Staff, R.A., Ellis, B.S., 2017. High-precision $^{40}Ar/^{39}Ar$ dating of pleistocene tuffs and temporal anchoring of the Matuyama–Brunhes boundary. Quat. Geochronol. 39, 1–23.

Marshall, B.D., DePaolo, D.J., 1982. Precise age determinations and petrogenetic studies using the K–Ca method. Geochim. Cosmochim. Acta 46, 2537–2545.

Marshall, B.D., DePaolo, D.J., 1989. Calcium isotopes in igneous rocks and the origin of granite. Geochim. Cosmochim. Acta 53, 917–922.

McIntosh, W.C., Chapin, C.E., 2004. Geochronology of the central Colorado volcanic field. New Mexico Bur. Geol. Miner. Resour. Bull. 160, 205–238.

Mills, R.D., Coleman, D.S., 2013. Temporal and chemical connections between plutons and ignimbrites from the Mount Princeton magmatic center. Contrib. Mineral. Petrol. 165, 961–980.

Mills, R.D., 2012. Re-Evaluating Pluton/Volcano Connections and Igneous Textures in Light of Incremental Magma Emplacement. Ph.D. Dissertation, University of North Carolina at Chapel Hill.

Moynier, F., Simon, J.I., Podosek, F.A., Meyer, B.S., Brannon, J., DePaolo, D.J., 2010. Ca isotope effects in Orgueil leachates and the implications for the carrier phases of ^{54}Cr anomalies. Astrophys. J. Lett., L7–L13.

Mutschler, F.E., Wright, E.G., Ludington, S., Abbott, J.T., 1981. Granite molybdenite systems. Econ. Geol. 76, 874–897.

Nash, Perkins M. E, B.P., Christensen, J.N., Lee, D.-C., Halliday, A.N., 2006. The Yellowstone hotspot in space and time: Nd and Hf isotopes in silicic magmas. Earth Planet. Sci. Lett. 247, 143–156.

Perry, F.V., DePaolo, D.J., Baldridge, W.S., 1993. Neodymium isotopic evidence for decreasing crustal contributions to Cenozoic ignimbrites of the western United States: implication for the thermal evolution of the Cordilleran crust. Geol. Soc. Am. Bull. 105, 872–882.

Pourmand, A., Dauphas, N., 2010. Distribution coefficients of 60 elements on TODGA resin: application to Ca, Lu, Hf, U and Th isotope geochemistry. Talanta 81, 741–753.

Rudnick, R.L., Gao, S., 2003. Composition of the continental crust. In: Treatise on Geochemistry, vol. 3, pp. 1–64.

Russell, W.A., Papanastassiou, D.A., Tombrello, T.A., 1978. Ca isotopes on the Earth and other solar system materials. Geochim. Cosmochim. Acta 42, 1075–1090.

Schiller, M., Paton, C., Bizarro, M., 2015. Evidence for nucleosynthetic enrichment of the protosolar molecular cloud core by multiple supernova events. Geochim. Cosmochim. Acta 149, 88–102.

Shannon, J.R., 1988. Geology of the Mount Aetna Cauldron Complex, Sawatch Range, Colorado. Ph.D. Thesis, Colorado School of Mines, Golden, Colorado,, p. 439.

Simon, J.I., 2000. A Petrogenetic Comparison of Early Crystal-Poor Ash-Flow Tuffs, San Juan Volcanic Field, south-central Colorado. MSc, Colorado School of Mines. 280 pp.

Simon, J.I., DePaolo, D.J., 2010. Stable calcium isotopic composition of meteorites and rocky planets. Earth Planet. Sci. Lett. 289, 457–466.

Simon, J.I., Reid, M.R., Young, E.D., 2007. Lead isotopes by LA-MC-ICPMS: tracking the emergence of mantle signatures in an evolving silicic magma system. Geochim. Cosmochim. Acta 71, 2014–2035.

Simon, J.I., DePaolo, D.J., Moynier, F., 2009. Calcium isotope composition of meteorites, Earth and Mars. Astrophys. J. 702, 707–715.

Simon, J.I., Weis, D., DePaolo, D.J., Renne, P.R., Mundil, R., Schmitt, A.K., 2014. Assimilation of preexisting Pleistocene intrusions at Long Valley by periodic magma recharge accelerates rhyolite generation: rethinking the remelting model. Contrib. Mineral. Petrol. 167, 955. https://doi.org/10.1007/s00410-013-0955-5.

Simon, J.I., Jordan, M.K., Tappa, M.J., Schauble, E.A., Kohl, I.E., Young, E.D., 2017. Calcium and titanium isotope fractionation in refractory inclusions: tracers of condensation and inheritance in the early solar protoplanetary disk. Earth Planet. Sci. Lett. 472, 277–288.

Sisson, T.W., Ratejeski, K., Hankins, W.B., Glazner, A.F., 2005. Voluminous granitic magmas from common basaltic sources. Contrib. Mineral. Petrol. 148, 635–661.

Stein, H.J., Crock, J.G., 1990. Late-Cretaceous–Tertiary magmatism in the Colorado mineral belt; rare earth element and samarium–neodymium isotopic studies. In: Anderson, J.L. (Ed.), The Nature and Origin of Cordilleran Magmatism, vol. 174. In: Geological Society of America Memoir, pp. 195–223.

Stelten, M.E., Cooper, K.M., Vazquez, J.A., Reid, M.R., Barfod, G.H., Wimpenny, J., Yin, Q.-z., 2013. Magma mixing and the generation of isotopically juvenile silicic magma at Yellowstone caldera inferred from coupling ^{238}U–^{230}Th ages with trace elements and Hf and O isotopes in zircon and Pb isotopes in sanidine. Contrib. Mineral. Petrol. 166, 587–613.

Tweto, O., Sims, P.K., 1963. Precambrian ancestry of the Colorado Mineral Belt. Geol. Soc. Am. Bull. 74, 991–1014.

Valdes, M.C., Moreira, M., Foriel, J., Moynier, F., 2014. The nature of Earth's building blocks as revealed by calcium isotopes. Earth Planet. Sci. Lett. 394, 135–145.

Vazquez, J.A., Reid, M.R., 2002. Time scales of magma storage and differentiation of voluminous high-silica rhyolites at Yellowstone caldera, Wyoming. Contrib. Mineral. Petrol. 144, 274–285.

Yokoyama, T., Misawa, K., Okano, O., Shih, C.-Y., Nyquist, L.E., Simon, J.I., Tappa, M., Yoneda, S., 2017. Extreme early solar system chemical fractionation recorded by alkali-rich clasts contained in ordinary chondrite breccias. Earth Planet. Sci. Lett. 458, 233–240.

Zimmerer, M.J., McIntosh, W.C., 2012. An investigation of caldera-forming magma chambers using the timing of ignimbrite eruptions and pluton emplacement at the Mt. Aetna caldera complex. J. Volcanol. Geotherm. Res. 245–246, 128–148.